Search for η_b in Run 1 J/ψ Data

THE CDF COLLABORATION

Abstract

The η_b is the $J^{PC} = 0^{-+}$ $b\bar{b}$ state analogous to the η_c observed in the charm sector. Its existence has not been confirmed by any experiment, though theorists have recently suggested that it could be observed at the Tevatron in Run 2 through its decay to $J/\psi J/\psi$. This article describes a search for this particle at CDF in Run 1 using this decay channel. A small peak has been found, with 7 events where 1.8 events are expected from background. The statistical significance is estimated to be 2.2σ, and an upper limit is set on the product of cross section and branching fractions.

1 Introduction

The development of the non-relativistic QCD (NRQCD) framework for understanding the bound states of heavy quarks and antiquarks was spurred, in part, by the CDF observation of what was then deemed an anomalously large direct $\psi(2S)$ cross section compared to prior theoretical models. [1] Subsequent models have taken into account higher-order effects than those explicit in the earlier models and isolate non-perturbative effects into factors called "NRQCD matrix elements" which must be determined experimentally. These parameters are universal and therefore relate predictions across different quarkonia species. Predictions concerning bottomonia are considered to be the most reliable, and with this in mind theorists have analyzed the CDF Υ [2] and χ_b [3] cross section measurements [4][5]. [5] predicts the η_b cross section and finds it to be roughly three to six times that of $\Upsilon(1S)$. The authors propose finding this particle through its decay to two J/ψ's; the branching fraction of this mode, however, can only be estimated to be between 7×10^{-5} and 7×10^{-3}. Experimental tests of these theoretical calculations will have to wait for the observation of other decay modes.

The mass of the η_b, however, is an important test of perturbative QCD in the $b\bar{b}$ system. An early estimate, using a potential model, of the hyperfine splitting between the $\Upsilon(1S)$ and the η_b was 57 MeV/c^2 [6], though it was recognized then that relativistic corrections were potentially quite large. A lattice gauge calculation in 1997 [7] gave a range of values between 44 and 89 MeV/c^2, though the prediction for the $\Upsilon(1S)$ mass was off by about 50 MeV/c^2. More recent lattice gauge results fix the $\Upsilon(1S)$ mass to the measured value and give mass splittings of 30 MeV/c^2 [8] and between 19 and 33 MeV/c^2 [9]. These more recent calculations predict an η_b mass in the range 9.427 to 9.441 GeV/c^2. Following the pattern of bottomonia widths as compared to those in charmonia, the natural width is expected to be narrower than the η_c width of $13.2^{+3.8}_{-3.2}$ MeV/c^2 [10].

In this article, the J/ψ dimuon data sample in which the search for the η_b is conducted is described, as well as the simulation used to model its decay. The second ("non-leading") J/ψ is then reconstructed, also through the dimuon channel. A small peak is observed in the expected mass window.

2 Data sample

The search for $\eta_b \to J/\psi J/\psi$ decays begins with the $J/\psi \to \mu^+\mu^-$ datasets from Run 1. Muon candidates are accepted from any of the central muon detector systems, which cover roughly $|\eta| < 1$. Muon stubs are required to be well matched to CTC tracks with SVX fits. A $J/\psi \to \mu^+\mu^-$ decay is reconstructed with an oppositely charged pair of muon candidates. After the first ("leading") J/ψ has been found, η_b candidates are reconstructed by adding the two muon tracks from the non-leading $J/\psi \to \mu\mu$ decay to the vertex of the leading J/ψ. The four tracks are then constrained using to come from a common vertex, and mass constraints to the world average J/ψ mass [10] are applied to both muon pairs. Since the η_b is only directly produced in the $p\overline{p}$ interaction and decays promptly, the four-track vertex is further constrained to lie close to the beam.

2.1 Signal Simulation

The behavior of η_b events is investigated using a Monte Carlo model of η_b production and decay in the detector. The production model follows that of the Υ, using the same p_T spectrum measured in the CDF data [2]. The rapidity is generated according to a uniform distribution between -3 and 3.

The angular distribution of the muons from $\eta_b \to J/\psi J/\psi$ decay is worked out from the fact that the η_b has $J^{PC} = 0^{-+}$ and the J/ψ has 1^{--}. The decay proceeds through a P wave, and the two J/ψ polarizations are aligned. The detector response is then simulated using a fast parameterized detector simulation. The cut $p_T > 2.2$ GeV/c is applied to the muons of the leading J/ψ to account for the gross effects of the $J/\psi \to \mu\mu$ trigger.

2.2 Optimization

A first attempt was made to search for the $\eta_b \to J/\psi J/\psi$ decay by requiring all four muons to be identified as central muon candidates, using the same matching and track quality requirements as on the muons in the leading J/ψ. No events survived the vertex quality cuts.

The non-leading J/ψ's, however, are softer than those generally used in other analyses, where the only J/ψ in the event is the triggering phenomenon. The acceptance for η_b events can be increased by requiring good muon identification on only one leg and pairing that muon with another track. This "fourth track" can therefore fall below the inherent p_T threshold of the muon chambers and outside of their geometric acceptance.

The p_T cut on the fourth track is optimized by comparing the Monte Carlo signal with a sample of events where the vertex constraint has been relaxed. It is expected that a major source of background in this analysis consists of b hadron pairs, one of which decays via $J/\psi X$; the looser vertex constraint effectively lets in more of this kind of background. As shown in Figure 1, the maximum S^2/B is achieved with a p_T cut at 0.8 GeV/c. At this threshold, the increased acceptance of removing the muon stub requirement from the fourth track is about a factor of seven.

The resulting mass distribution is shown in Figure 2. The typical mass uncertainty estimated by the vertex fit is about 10 MeV/c^2, which is used as the bin size. A peak is seen around 9.44 GeV/c^2, with 9 events in four consecutive bins from 9.42 to 9.46 GeV/c^2 (the search window, defined in Section 2.4, is 9.36 to 9.46 GeV/c^2).

2.3 Comparison with Υ events

It is expected that η_b events look much like $\Upsilon(1S) \to \mu\mu$ events, aside from replacing the two muons with two J/ψ's. In particular, their underlying events are expected to be similar; it is therefore possible to compare the isolation characteristics of the η_b candidates with those of $\Upsilon(1S)$ candidates. The $\Upsilon(1S)$ candidates can also be used as a model of η_b to optimize selection criteria based on those characteristics.

The same quality cuts employed on the J/ψ's in the η_b search are applied to the high-mass dimuon dataset to find $\Upsilon \to \mu\mu$ events. An example of the mass spectrum, showing clear peaks for $\Upsilon(1S)$, $\Upsilon(2S)$, and $\Upsilon(3S)$, is shown in [2]. The underlying event is examined by looking at only $\Upsilon(1S)$ events, where the signal region is defined as the dimuon mass region between 9.2 and 9.6 GeV/c^2, and the sideband regions are defined as the surrounding regions between 9.0 and 9.8 GeV/c^2. Several quantities were explored, but the most effective one was found to be the scalar sum of p_T's of tracks in cones of $\Delta R < 0.4$ around, but not including, the two daughter muons. This cut is particularly useful in rejecting events where the daughters are associated with b jets. Figure 3 shows the spectrum for the signal and sideband regions, as well as the sideband-subtracted spectrum.

The distributions of the quantity in the SVX $\mu\mu\mu$+track signal and sideband regions can be seen in Figure 4. The directions of the Υ daughter muons are replaced by the directions of the η_b daughter J/ψ's. With such few events under consideration, their consistency with Figure 3 is difficult to gauge.

A selection criterion using this quantity can be optimized in a manner similar to that used before for the fourth track p_T cut. In this case, the signal is modeled by the sideband-subtracted $\Upsilon(1S)$ distribution, while the background denominator is given by the loose-cut data described in Section 2.2. The best upper limit is shown in Figure 5 to be 1.8 GeV/c. This cut preserves 88% of the signal. The resulting mass distribution of applying this additional criterion is shown in Figure 6.

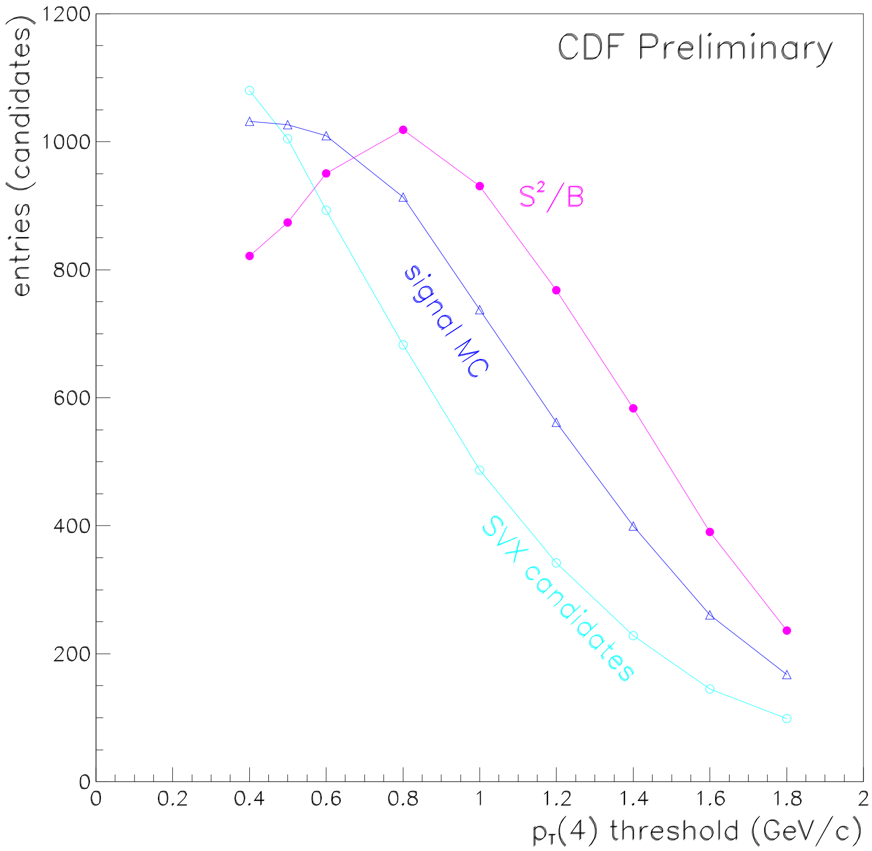

Figure 1: S^2/B for SVX $\mu\mu\mu$+track events as a function of the p_T cut on the track.

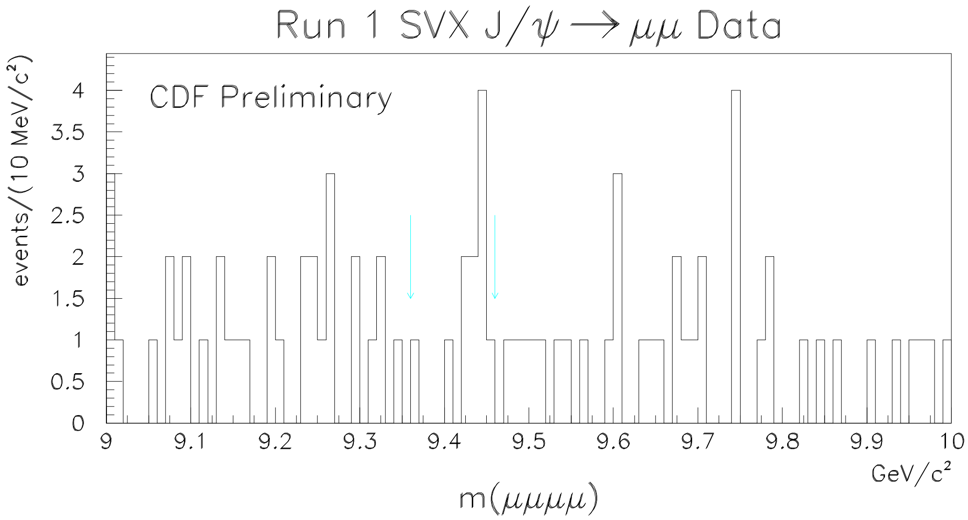

Figure 2: Mass distribution for SVX $\mu\mu\mu$+track candidates. The search window is marked by the arrows.

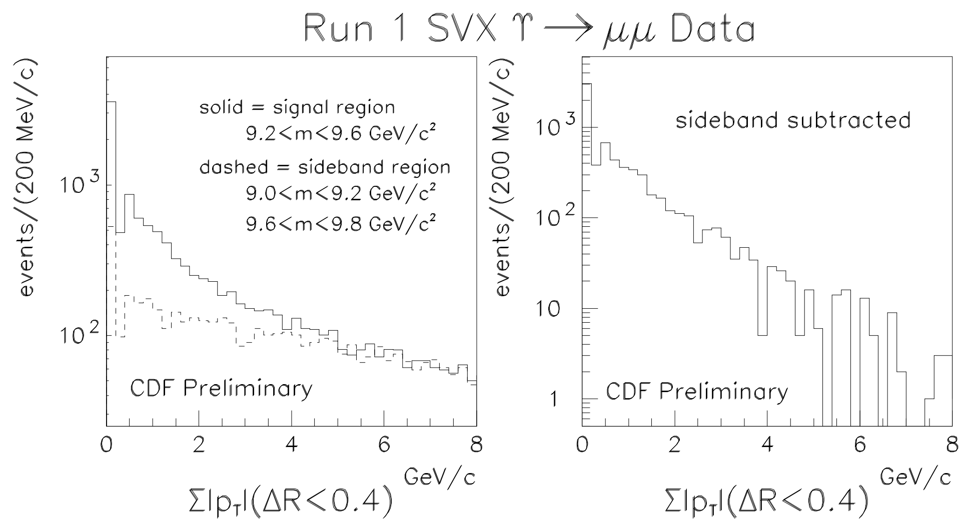

Figure 3: Scalar p_T sums in $\Delta R < 0.4$ cones around the two muons from SVX $\Upsilon(1S) \to \mu\mu$ decays.

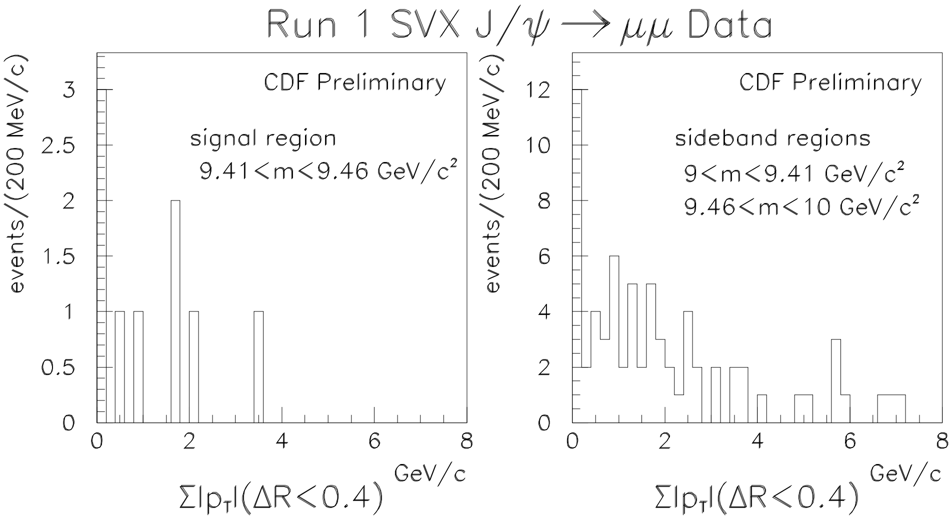

Figure 4: Scalar p_T sums in $\Delta R < 0.4$ cones around the two J/ψ's in SVX events.

2.4 Signal significance

The probability that the background can mimic the peak is a measure of the significance of the observation. The background level is treated as a Poisson-fluctuating variable and is determined by the sidebands.

The search window is defined to be between 9.36 and 9.46 GeV/c^2, which includes all the mass predictions in Section 1, though the more recent predictions [8][9] tend to fall on the high end of this window. The upper bound is also the mass of the $\Upsilon(1S)$ itself, which is expected to be more massive than the η_b. The sidebands are the mass regions between 9 and 10 GeV/c^2 excluding the search window.

The cluster width is taken to be 4 bins, which encompasses most of a cluster of events with mass resolution around 10 MeV/c^2. A toy Monte Carlo is used to determine the fraction of 100,000 trials which have 7 or more events clustered in 4 consecutive bins within the search window of 10 bins, resulting in a probability of 1.5%, or roughly equivalent to 2.2σ.

2.5 Mass

Assuming that the cluster of events in Figure 6 results from the production and decay of η_b to two J/ψ's, an unbinned likelihood fit can be applied to perform a simple calculation of its mass without energy loss corrections. The likelihood function consists simply of a gaussian signal and flat background distribution. The distribution in Figure 6 is, however, too small for a well-behaved fit, and the larger sample in Figure 2, before the isolation cut, is used instead. The fitted mass is $9445 \pm 6(stat)$ MeV/c^2.

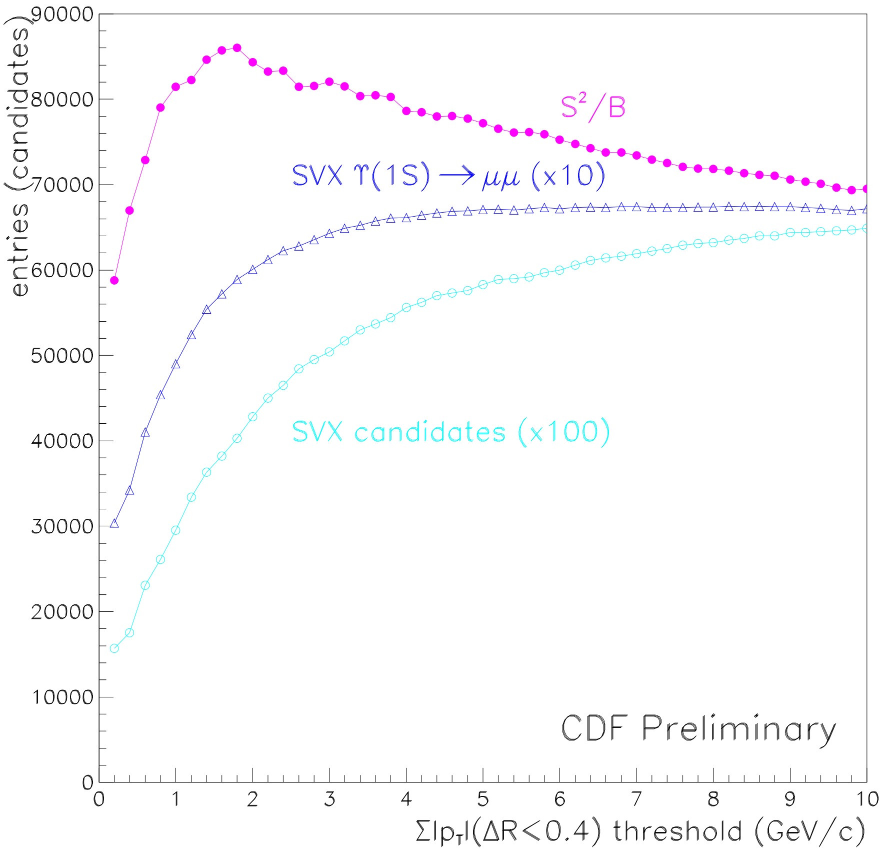

Figure 5: Scalar p_T sum threshold optimization in $\Delta R < 0.4$ cones around the bottomonia daughters.

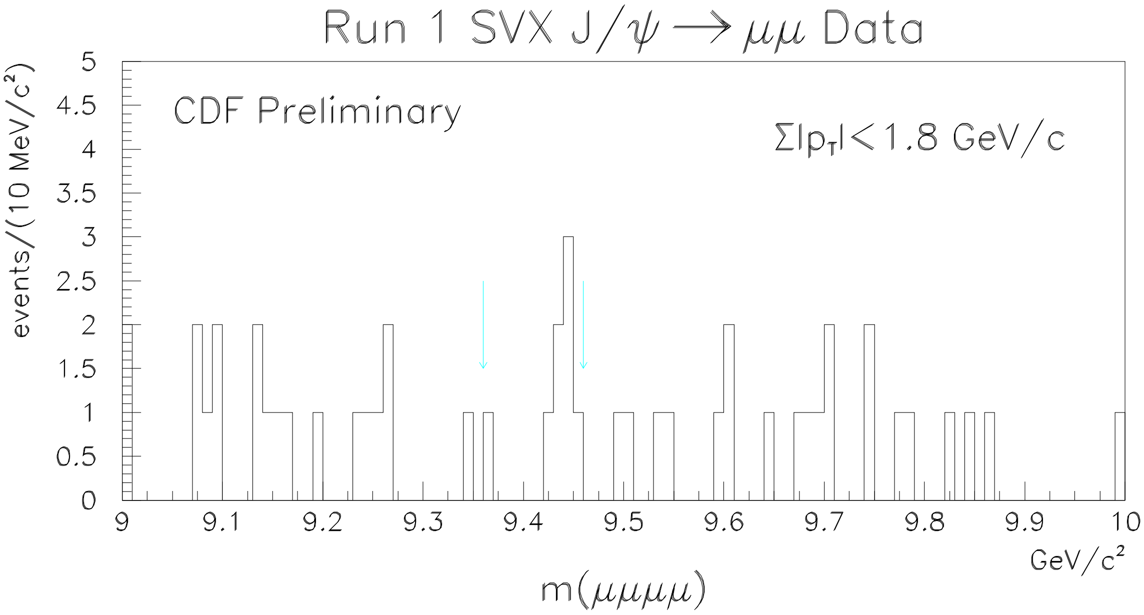

Figure 6: Mass distribution of $\mu\mu\mu$+track candidates after applying the optimized isolation cut.

3 Rate Limit

In light of the small peak, an upper limit is calculated for η_b production and decay to $J/\psi J/\psi$. Additional selection criteria are necessary in order to reliably quantify acceptance and efficiencies, and are chosen to follow those of the Run 1 $B^+ \to J/\psi K^+$ cross section [11] wherever possible. Only Run 1B data is used, and the events must have fired a selected dimuon trigger. Stricter requirements on the acceptance are applied, including limiting the identified muons to those found in the most central muon chambers, which cover $|\eta| < 0.6$. No isolation requirement is used. The resulting mass distribution is shown in Figure 7. One event is observed in the signal mass window.

3.1 Limit calculation

The product of η_b cross section and branching fractions is

$$\sigma_{\eta_b}(|y| < 0.4)\mathcal{B}(\eta_b \to J/\psi J/\psi)[\mathcal{B}(J/\psi \to \mu\mu)]^2 = \frac{N}{\mathcal{L} A_{MC}\epsilon_{trig}\epsilon_{rec}} \tag{1}$$

where N is the number of events observed, $\mathcal{L}$ is the integrated luminosity of the Run 1B data sample, A_{MC} is the acceptance calculated with simulation, and ϵ_{trig} and ϵ_{rec} are the trigger and reconstruction efficiencies not included in the simulation. With one event observed, and

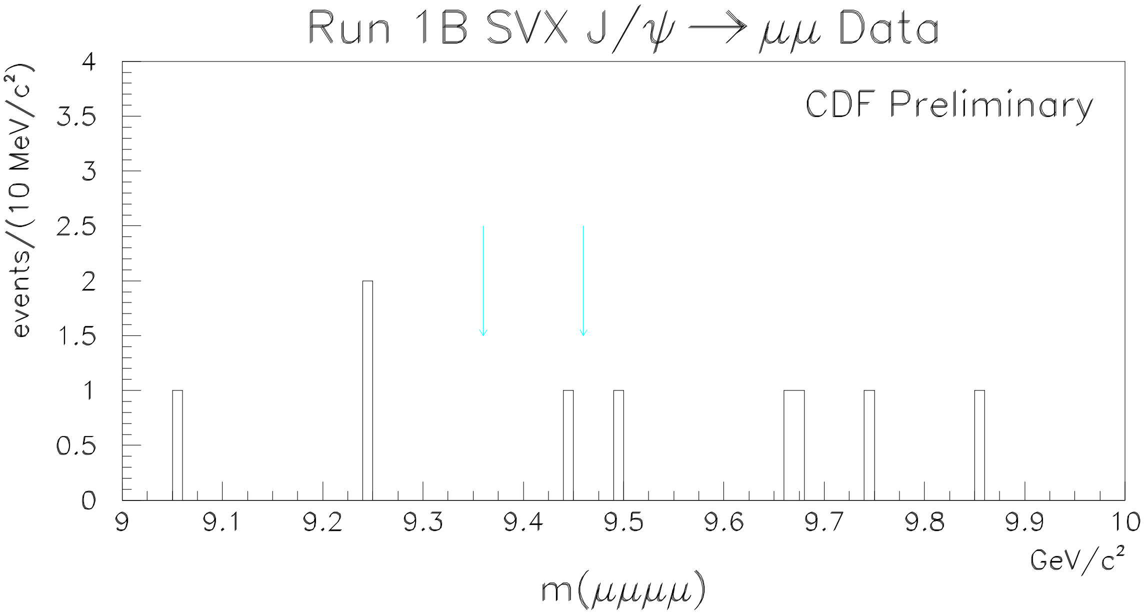

Figure 7: Mass distribution of $\mu\mu\mu$+track candidates after applying selection criteria for measuring the the cross section.

assumed to be signal for the purposes of the rate limit calculation, N is taken to be 5.14 events to obtain the 95% C.L. upper limit [10].

The luminosity $\mathcal{L}$ is the product of the following factors:

- the Run 1B integrated luminosity, 78.5 ± 3.2 pb^{-1}
- a correction factor for the time dependence in the measured J/ψ cross section, 0.88 ± 0.04
- a correction factor for the visible luminosity given the restricted acceptance.

The Monte Carlo acceptance A_{MC} is calculated using the simulation described in Section 2.1 to be $A_{MC} = 0.0095 \pm 0.0002$.

The trigger and reconstruction efficiencies not included in the simulation are summarized in Table 1. The trigger efficiency factor ϵ_{trig} accounts for Level 3 tracking and muon matching efficiency for the J/ψ trigger path. The reconstruction efficiency ϵ_{rec} includes the CTC tracking efficiency for tracks with $p_T > 0.8$ GeV/c and CTC exit radius $R_{exit} > 130$ cm, as well as efficiencies for central muon reconstruction and track matching.

The SVX fraction, following the method of [11], is the fraction of J/ψ's reconstructed with CTC tracks which are also reconstructed with SVX fits. The vertex constraint, described in Section 2, is taken to be $(99 \pm 1)\%$ efficient as designed.

If the single event observed in the signal region is assumed to be signal, then Equation 1, using the corrected integrated luminosity and trigger and reconstructed efficiencies, gives as

factor	description	efficiency
ϵ_{trig}	L3 CTC tracking	0.97 ± 0.02
	L3 track-muon linking	0.998 ± 0.002
ϵ_{rec}	offline CTC tracking	$(0.996 \pm 0.009)^4$
	offline muon reconstruction	$(0.980 \pm 0.010)^3$
	offline J/ψ track-muon matching	0.987 ± 0.010
	third track-muon matching	0.9933 ± 0.0014
	SVX fraction	0.532 ± 0.002
	vertex χ^2 cut	0.99 ± 0.01

Table 1: Efficiencies and acceptances for the rate limit calculation. The method of evaluating the SVX fraction is based on [11].

		relative %
luminosity	Run 1B	± 4.1
	correction	± 5
	z vertex correction	± 1.2
L3 trigger	CTC tracking efficiency	± 2
	track-muon linking	± 0.2
offline	CTC tracking efficiency	± 3.6
	muon reconstruction	± 3.1
	J/ψ track-muon matching	± 1.0
	third track-muon match	± 0.14
	SVX fraction	± 0.38
	vertex χ^2 cut	± 1
Monte Carlo	sample size	± 2
	b	± 4
	m, n	± 2
	trigger simulation	± 6

Table 2: Systematic uncertainties, in relative percentage, in the rate limit calculation.

the product of cross section and branching fractions 3.5 pb. The 95% C.L. upper limit on the product is calculated to be 18 pb.

3.2 Systematic uncertainties

The systematic uncertainties in the rate limit are summarized in Table 2. Most arise from uncertainties in the measurements of acceptance and efficiencies in Section 3.1. The uncertainties due to the η_b production spectrum used in the simulation are evaluated by varying the spectrum parameters (listed as b and m and n, the latter two being highly correlated). The trigger simulation introduces a systematic uncertainty of $\pm 6\%$, computed using the $\pm 1\sigma$ variations in the Level 1 and Level 2 efficiency parameterizations. The total relative systematic uncertainty is 11%.

3.3 Comparison with theory

The expected range of the η_b cross section is roughly three to six times that of $\Upsilon(1S)$, and the branching fraction to $J/\psi J/\psi$ is between 7×10^{-5} and 7×10^{-3}. The integrated $\Upsilon(1S)$ cross section and $\Upsilon(1S) \to \mu\mu$ branching fraction has been measured at CDF to be 690 pb. Using the PDG branching fractions [10]

$$\begin{aligned} \mathcal{B}(J/\psi \to \mu\mu) &= (5.88 \pm 0.10)\% \\ \mathcal{B}(\Upsilon(1S) \to \mu\mu)) &= (2.48 \pm 0.06)\%, \end{aligned}$$

the range on the product of cross section and branching fractions, $\sigma_{\eta_b}(|y| < 0.4)\mathcal{B}(\eta_b \to J/\psi J/\psi)[\mathcal{B}(J/\psi \to \mu\mu)]^2$, is 0.02 to 4 pb. The 95% C.L. limit of Section 3.1 is above the upper range, though if the single observed event is indeed signal, the observed rate would be just within the upper expected range.

4 Variations

A number of checks of the peak have been performed, and the peak has been found to be reasonably robust against changes in the selection criteria. It is also instructive to examine the mass distribution of the non-leading dimuons to see whether they cluster near the J/ψ mass, as described in Section 4.1, and to search for additional events by looking for non-leading $J/\psi \to ee$ decays as described in Section 4.2.

4.1 Non-leading J/ψ mass

In order to examine the non-leading dimuon mass, the events are refit requiring only the leading J/ψ to be mass constrained. For the second J/ψ a similar correction can be effected by taking the mass difference between the four-muon combination and that of the non-leading J/ψ and adding back the world-average J/ψ mass.

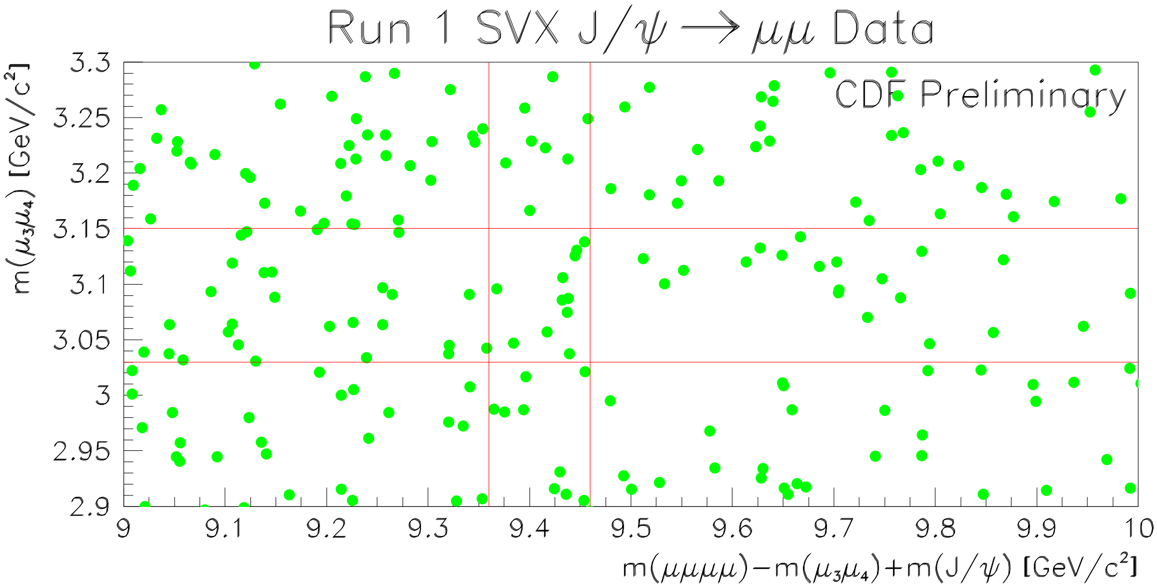

Figure 8: $\mu\mu\mu$+track plotted versus the non-leading J/ψ candidate mass, with signal mass regions marked.

Figure 8 shows the corrected $\mu\mu\mu$+track mass against the mass of the non-leading J/ψ candidate. The search window for η_b's is marked by the vertical lines, while the horizontal lines delimit the (non-leading) dimuon mass window between 3.03 and 3.15 GeV/c^2. A cluster of events can be seen on the right side of the intersection of the two windows.

Figure 9 shows the mass distribution of the non-leading J/ψ in the search window for η_b's and the corrected four-muon mass distribution for events in the non-leading J/ψ mass window.

4.2 Investigations with $J/\psi \to e^+e^-$

An analysis has been made of dimuon-triggered events where a non-leading J/ψ is reconstructed using two electron candidates. The general method of Section 2 is followed, except that electron instead of muon requirements are used for one daughter of the non-leading J/ψ, while the other daughter is subject to more inclusive criteria.

Following the spirit of the nominal analysis, one electron is identified using the soft lepton tagging (SLT) criteria developed for previous mixing analyses [12] while the other uses looser criteria. Muon stub-linked tracks are excluded from consideration as electrons, and both must also have energy loss dE/dx, calculated with an electron mass hypothesis, consistent with that of an electron. For the SLT-tagged electron, the p_T threshold is optimal at 1.6 GeV/c while the p_T threshold for the non-tagged track is kept at 0.8 GeV/c as before.

The decay is simulated using the method described in Section 2.1, where the SLT track

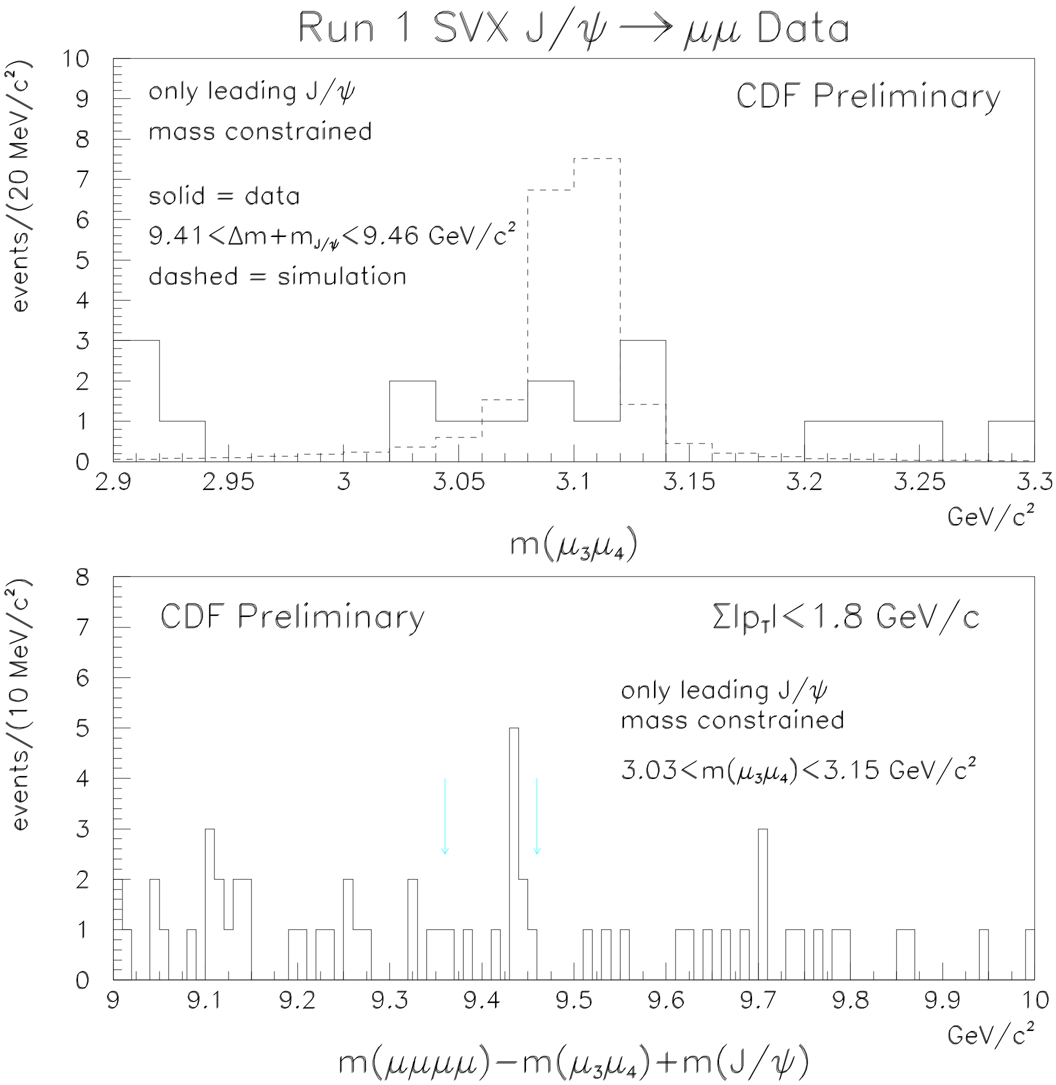

Figure 9: Top: mass distribution of the non-leading J/ψ for SVX data in the $\mu\mu\mu$+track signal region (solid), compared with the corresponding simulated mass distribution (dashed). Bottom: $\mu\mu\mu$+track mass distribution of SVX data after the mass window selection on the non-leading J/ψ.

is required to be in the CES fiducial region.

Bremsstrahlung effects produce a long low tail in the e^+e^- mass distribution, as shown in Figure 10(top left). This effect also produces a long tail and broad peak in the resulting $\mu\mu ee$ distribution in Figure 10(top right), though the impact is reduced in this distribution by a minimum ee mass requirement of 2.8 GeV/c^2, which is later applied to data as well. A correction can be applied in the manner of Section 4.1, subtracting the ee mass from the $\mu\mu ee$ mass and adding back the world-average J/ψ mass. The resulting narrower mass distribution is shown in Figure 10(bottom left). For comparison, the $\mu\mu ee$ mass distribution with both J/ψ's mass constrained is shown in the bottom right plot; it is narrower but with a 5% efficiency loss for events which end up in the peak, defined as those events with masses above 9.41 GeV/c^2. The overall efficiency loss, including the tail, is 12%. The corrected mass (bottom left) is used in this analysis.

Based on the peak observed in Figure 2, along with the relative yield of $\mu\mu e$+track and $\mu\mu\mu$+track events and the electron identification efficiency on the third track, approximately one event is expected to be found. The actual mass distribution in SVX data is shown in Figure 11. The mass window on the dielectron pair is 2.8 to 3.15 GeV/c^2. No distinct signal peak is observed in the mass distributions, consistent with the expectation.

The result of combining the electrons with the corresponding muon analysis variant, mass-constraining only the leading J/ψ and using the corrected total mass, is shown in Figure 12. The combined scatter plots of the non-leading dilepton mass against the corrected mass are shown in Figure 13. The few events which contribute to the combined cluster fall on the low side of the J/ψ mass. This behavior would not be surprising for such a small sample of true signal events, given the long radiative tail of the $J/\psi \to ee$ decays.

4.3 Summary of Variations

Table 3 summarizes the effects of the analysis variations investigated in this section, giving event yields in the mass distributions and in the search window, as well as the significance calculation. The analysis variations have shown that the behavior of the peak observed in Figure 2 is robust against cut variations. An examination of the non-leading J/ψ masses of the η_b candidates also reveals a cluster of events near the expected mass, behavior which shows further consistency with η_b decay. A search using the $J/\psi \to ee$ decay has also been performed and is combined with the $\mu\mu\mu$+track analysis. While the combination improves the apparent significance of the signal, it should be taken as supporting the hypothesis of η_b production at CDF rather than confirming it.

5 Conclusion

A search has been made for the η_b through its decay to two J/ψ's in Run 1 $J/\psi \to \mu\mu$ data. A small peak is observed, with 7 events in the search window where 1.8 background events are expected based upon the mass sidebands. The probability that the peak could be a background fluctuation is assessed to be 1.5%, or about 2.2σ. A simple fit to the mass

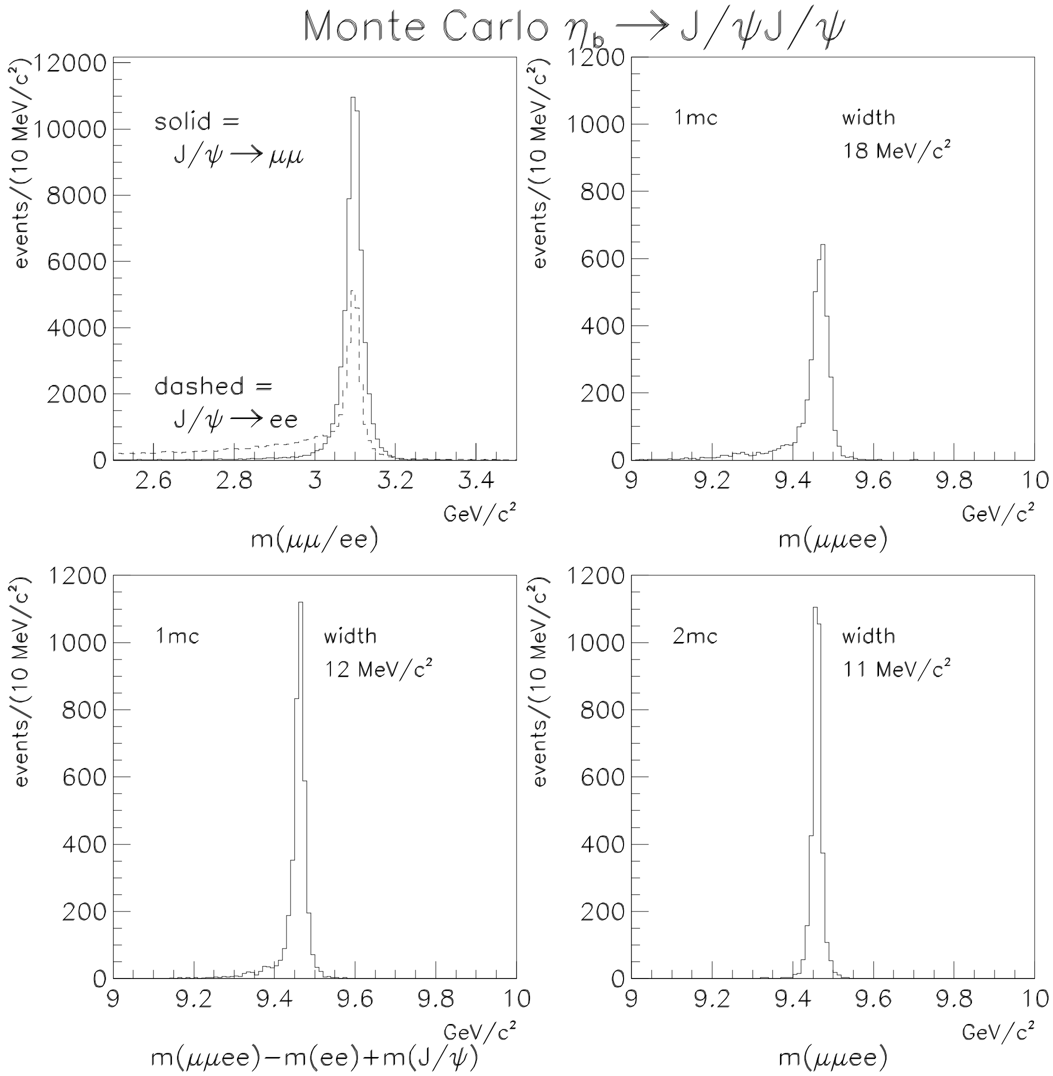

Figure 10: Top left: simulated dilepton mass distributions in $\eta_b \to J/\psi J/\psi$ decay. The solid histogram shows the (triggering) $J/\psi \to \mu\mu$, while the dashed histogram shows the mass distribution of $J/\psi \to ee$ with the long bremsstrahlung tail. Top right: raw mass distribution with the J/ψ mass constraint applied only to the muon pair. Bottom left: mass with the "corrected" $J/\psi \to ee$. Bottom right: comparison with $\mu\mu ee$ mass after applying mass constraints to both J/ψ's.

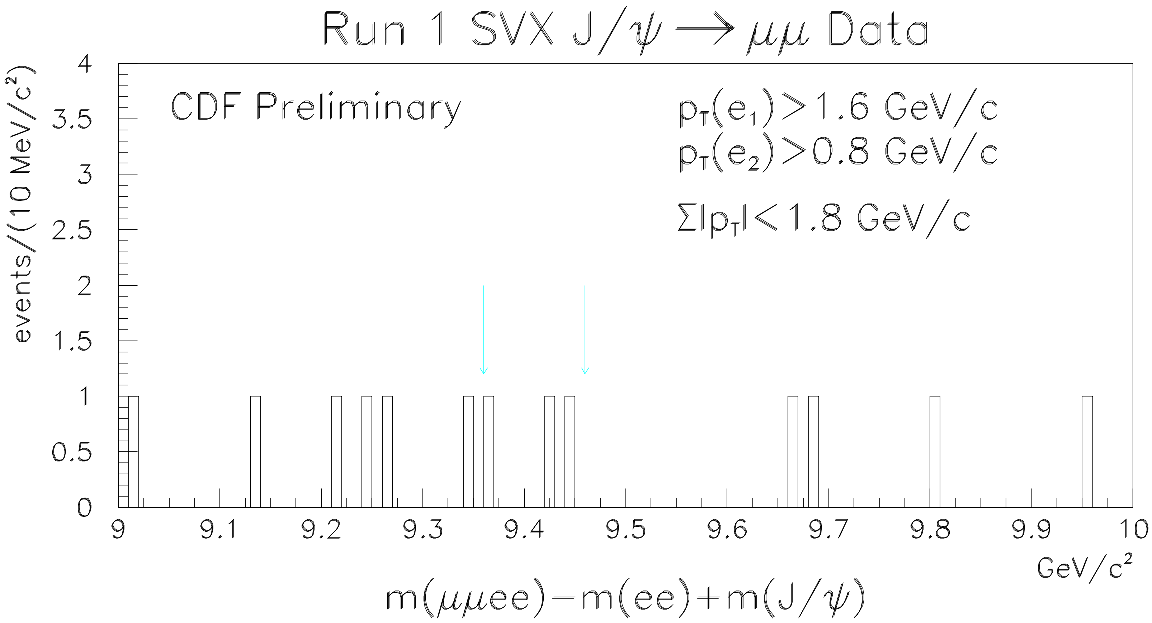

Figure 11: mass distribution of $\mu\mu ee$ candidates following the isolation cut, where one electron is identified with soft-lepton requirements and the other as a track. The ee mass is required to fall between 2.8 and 3.15 GeV/c^2.

	Fig.	Total evts (100 bins)	Signal (4/10 bins)	Prob. (%)	σ
SVX	2	81	9	2.8	1.9
iso (nom.)	6	48	7	1.5	2.2
$\Delta m + M_{J/\psi}$ iso	9	60	8	1.2	2.3
$\mu\mu + ee$ iso	12	73	10	0.31	2.7

Table 3: Yields and Poisson probabilities, with Poisson-varying background levels, for different selection criteria investigated in this report. The total mass window extends from 9 to 10 GeV/c^2, while the search window covers 10 bins between 9.36 to 9.46 GeV/c^2. The probability is calculated for a 4-bin cluster in the search window.

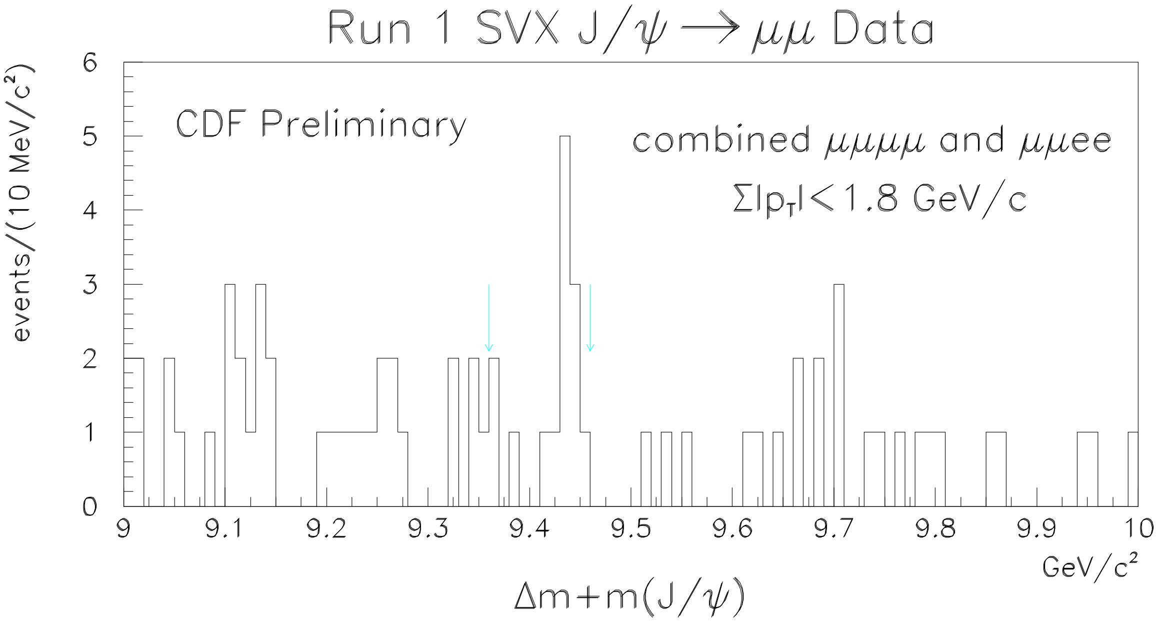

Figure 12: mass distribution of $\mu\mu\mu\mu$ and $\mu\mu ee$ candidates following the isolation cut, where one lepton is identified with muon chamber or soft-electron requirements and the other as a track.

distribution gives $9445 \pm 6(stat)$ MeV/c^2 as the mass of the peak, where the error is only statistical. This central value is consistent with recent predictions using lattice calculations of NRQCD matrix elements. Moreover, the non-leading dimuon masses cluster near the J/ψ mass, as expected for an η_b signal, and the addition of dielectron pairs also supports the hypothesis of signal. Since the peak is small, however, a 95% C.L. upper limit on the product of cross section and branching fractions is calculated, giving $\sigma\eta_b(|y| < 0.4)\mathcal{B}(\eta_b \rightarrow J/\psi J/\psi)[calB(J/\psi \rightarrow \mu\mu)]^2 < 18$ pb^{-1} with an 11% relative systematic uncertainty. This limit is above the theoretical range of 0.02 to 4 pb^{-1}, though the single event which survives the more restrictive cuts is consistent with the upper part of that range.

In tandem with this analysis, confirmation of this signal is already being pursued in Run 2 data. The lower p_T threshold of the central muon trigger, combined with the extended SVX coverage, promises to confirm this signal with 100 pb^{-1} of integrated luminosity. This luminosity appears to be achievable before the end of 2002.

References

[1] F. Abe *et al.*, *Phys. Rev. Lett.* **79**, 572 (1997).

[2] F. Abe *et al.*, *Phys. Rev. Lett.* **75**, 4358 (1995); D. Acosta *et al.*, *Phys. Rev. Lett.* **88**, 161802 (2002)

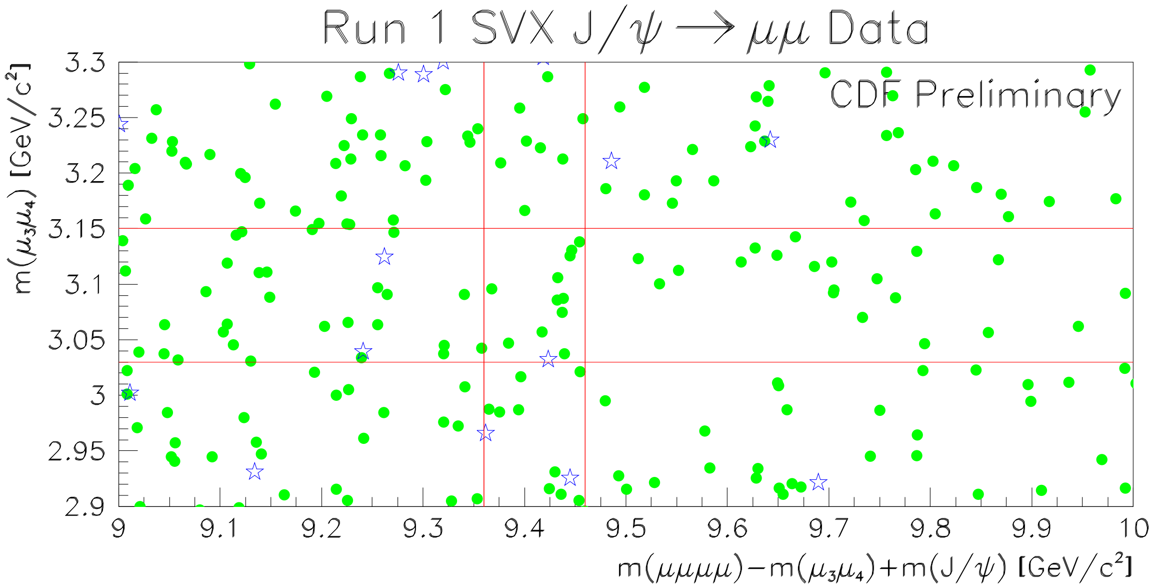

Figure 13: Combined scatter plot of non-leading J/ψ candidate masses versus the corrected total mass, with the signal regions marked. Solid points are muon events, while stars are electron events. The isolation cut was applied.

[3] F. Abe *et al.*, *Phys. Rev. Lett.* **84**, 2094 (2000).

[4] P. Cho, A. Leibovich, *Phys. Rev.* **D53**, 150 (1996); *Phys. Rev.* **D53**, 6203 (1996).

[5] E. Braaten, S. Fleming, A.K. Leibovich, *Phys. Rev.* **D63**, 094006 (2001).

[6] J.L. Rosner, in S.J. Lindenbaum, ed., *Experimental Meson Spectroscopy - 1983*, AIP Conference Proceedings No. 113 (New York: AIP, 1984), p. 46.

[7] G.S. Bali, K. Schilling, A. Wachter, *Phys. Rev.* **D56**, 2566 (1997); F.J. Ynduráin, "QCD: Perturbative or Nonperturbative," *Lectures at the XVII International School of Physics* (Lisbon, 1999), FTUAM 99-32.

[8] A. Spitz, H. Hoeber, N. Eicker, S. Güsken, Th. Lippert, K. Schilling, T. Struckmann, P. Ueberholz, J. Viehoff, hep/lat-9906009, 14 June 1999.

[9] T. Manke *et al.*, *Phys. Rev.* **D62**, 114508 (2000).

[10] D.E. Groom *et al.*, *Eur. Phys. J.* **C15**, 1 (2000).

[11] D. Acosta *et al.*, *Phys. Rev.* **D65**, 052005 (2002).

[12] F. Abe *et al.*, *Phys. Rev.* **D60**, 072003 (1999).